Title: Polarimetry of 16Ngs produced in mu --capture on 16O nuclei

Author: C.P. Bee, D. Conti, M. Hadri, S. Kistryn, J. Lng, O. Naviliat-Cuncic, Elżbieta Stephan, Wiktor Zipper

Citation style: Bee C.P., Conti D., Hadri M., Kistryn S., Lng J., Naviliat-Cuncic O., Stephan Elżbieta, Zipper Wiktor. (1997). Polarimetry of 16Ngs produced in mu --capture on 16O nuclei. "Acta Physica Polonica. B" (1997, no. 7, s. 1659-1676).

UNIWERSYTET ŚLĄSKI W KATOWICACH · Biblioteka Uniwersytetu Śląskiego · Ministerstwo Nauki i Szkolnictwa Wyższego

POLARIMETRY OF $^{16}N_{gs}$ PRODUCED IN μ^--CAPTURE ON ^{16}O NUCLEI

C.P. Bee, D. Conti, M. Hadri, St. Kistryn [*], J. Lang,
O. Naviliat-Cuncic, J. Sromicki, E. Stephan [**]

Institut für Teilchenphysik, Eidgenössische Technische Hochschule
Zürich, Switzerland

K. Bodek, J. Smyrski, A. Strzałkowski, J. Zejma

Institute of Physics, Jagellonian University, Cracow, Poland

L. Grenacs

Université Catholique de Louvain, Belgium

R. Abela, P. Böni, F. Foroughi

Paul Scherrer Institut, Villigen, Switzerland

W. Zipper

Institute of Physics, University of Silesia, Katowice, Poland

AND A. Proykova

Institute of Physics, University of Sofia, Bulgaria

A polarimetry technique based on stack targets and β-γ-coincidences has been applied to the ^{16}N nuclei produced in the ground state capture of negative muons on ^{16}O nuclei. The performance of the polarimeter and the first measurements of β-asymmetry due to the longitudinal nuclear polarization are discussed.

PACS numbers: 24.80. +y, 13.88. +e, 14.60. Ef, 2340. -s

[*] On leave of absence from Institute of Physics, Jagellonian University, Cracow.
[**] On leave of absence from Institute of Physics, University of Silesia, Katowice.

1. Motivation

Tests of time-reversal violation (TRV) and investigation of hadronic effects in nuclear media are two interesting applications of muon capture reactions on light nuclei which involve polarization of the final nucleus. They are discussed briefly in the following.

Violation of CP-symmetry has been observed up to now only in the decay of neutral K mesons [1]. This phenomenon, and the closely related time-reversal violation (TRV), can be incorporated into the standard model (SM), however, its origin is not yet understood. Extensive experimental efforts to find TRV in other systems with the expectation that it will require the introduction of "new physics" have failed, although most experiments have not yet reached the required accuracy. New high precision measurements are needed to test the numerous extensions of the SM. Up to now the search for TRV in semileptonic systems without strangeness has focused on two kinds of experiments: *(i)* search for neutron and atomic electric dipole moments [2], *(ii)* triple correlation measurements in neutron and nuclear β-decay [2,3]. The muonic sector has remained completely unexplored, apart from the pure leptonic decay where a null result was found [4].

If the magnitude of the TRV effects would scale up with the mass of the lepton involved, as some theorists anticipate, the muon capture reaction

$$\mu^- + {}^A_Z X \longrightarrow {}^A_{Z-1} Y + \nu_\mu \tag{1}$$
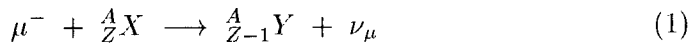
might be advantageous compared to β-decay. Additionally, the high momentum transfer (~ 80 MeV/c) may cause an enhancement of TRV by induced couplings. Furthermore, the final-state interaction which may obscure the TRV signal in β-decay experiments is not present here. The observable of interest is the transverse polarization of the final nucleus (P_T). Its nonzero value would signal unambiguously TRV. A result consistent with zero could be used to deduce limits on exotic interactions which violate time-reversal symmetry.

Another field where muon capture may serve as a testing ground is the investigation of the hadronic effects in nuclear media. The outstanding problem here is whether the nucleon form factors are modified when the nucleon is embedded into nuclear matter [5]. The most accurate experimental value of the ratio g_P/g_A (pseudoscalar/axial vector) for the ground-state capture on ^{12}C does not confirm this expectation. The adequacy of this result may be however criticized, because the main contribution to the reaction amplitude comes from the peripheral p-shell nucleons which are only weakly influenced by the nuclear matter. The capture on ^{16}O necessarily involves the d-shell nucleon and thus can deliver a different piece of information. Recently, this

problem became exciting again, since new calculations, involving the phenomenological Lagrangian with the QCD-symmetries imposed, predict no scaling of the g_P/g_A-ratio [6,7]. The accurate determination of g_P/g_A could be obtained *e.g.* from a measurement of the longitudinal (P_L) and average (P_{av}) polarization of the final nucleus. The simultaneous measurement of P_L and P_{av} was performed only in the case of μ^--capture on ^{12}C [8].

From the above considerations it can be concluded that the polarization of the final nucleus in ordinary muon capture is an important and very interesting quantity. In the following we describe an attempt to measure the polarization observables of the ^{16}N nucleus produced in the ground-state capture of negative muons on ^{16}O nuclei:

$$\mu^- + {}^{16}O \longrightarrow {}^{16}N_{gs} + \nu_\mu. \tag{2}$$
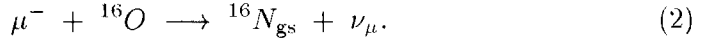
2. Polarization observables

The vector component of the final nucleus spin $\vec{J}_N$ can be described in terms of three polarization observables:

1. average polarization

$$P_{av} \equiv P_\mu \cdot \langle \hat{J}_N \cdot \hat{\sigma}_\mu \rangle, \tag{3}$$

2. longitudinal polarization

$$P_L \equiv \langle \hat{J}_N \cdot \hat{v}_N \rangle, \tag{4}$$

3. transverse polarization

$$P_T \equiv P_\mu \cdot \langle \hat{J}_N \cdot (\hat{\sigma}_\mu \times \hat{v}_N) \rangle, \tag{5}$$

where $\hat{J}_N = \vec{J}_N/J_N$ and $\hat{v}_N$ are the spin and the recoil directions of the final nucleus. P_μ and $\hat{\sigma}_\mu$ describe the muon polarization and the muon spin direction at the instant of capture, respectively.

The fixed helicity of the muon neutrino (-1) restricts the number of amplitudes describing the reaction (2) in the recoil nucleus frame to two independent components. In the notation of Hwang and Primakoff [9] we have:

$$M_{-1/2} = F_A \cdot \left(1 + \hat{F}_M \cdot \frac{E_\nu}{2m}\right)$$

$$M_{+1/2} = F_A \cdot \left(1 + \tilde{F}_P \cdot \frac{m_\mu E_\nu}{m_\pi^2} - \tilde{F}_E \cdot \frac{E_\nu}{2m}\right), \tag{6}$$

where F_A, F_P, F_M and F_E are the axial, pseudoscalar, weak magnetic and weak electric nuclear form factors, respectively (and $\tilde{F}_i = F_i/F_A$). E_ν is the neutrino energy, m_μ is the muon mass and m is the proton mass. The subscripts $\pm 1/2$ designate the helicity of the final state $(^{16}N_{gs} + \nu_\mu)$ in the recoil frame. Thus, $M_{-1/2}$ $(M_{+1/2})$ stands for a recoil nucleus with magnetic quantum number $M = -1$ $(M = 0)$ in that frame. The polarization observables: P_{av}, P_L and P_T depend on X, the ratio of $M_{-1/2}$ vs. $M_{+1/2}$. For our reaction (2) we have:

$$P_{av} = P_\mu \cdot \frac{2}{3} \cdot \frac{1 + 2\sqrt{3}X}{2 + X^2},$$
$$P_L = \frac{-1}{2 + X^2}. \tag{7}$$

The transverse polarization of the final nucleus P_T changes sign under time reversal and thus should vanish if time reversal holds. P_T may be expressed in terms of the relative phase ϕ_{+-} between the two contributing complex amplitudes. The angle ϕ_{+-} is a measure of the departure from the V-A theory. For spinless targets P_T can be estimated as [10]

$$P_T \approx \frac{1}{4} \cdot P_\mu \cdot \sqrt{J_N(J_N + 1)} \cdot \sqrt{|P_L| \cdot (1 - |P_L|)} \cdot \sin\phi_{+-}, \tag{8}$$

and thus

$$P_T \approx \frac{\sqrt{6}}{4} \cdot P_\mu \cdot \frac{\sqrt{1 + X^2}}{2 + X^2} \cdot \sin\phi_{+-}. \tag{9}$$

When time reversal holds the amplitudes are relatively real, *i.e.* they differ in phase by 0 or π.

3. Experiment

3.1. Principle of measurement

From the definitions (3)–(5) it can be seen that for a measurement of P_{av} the muon must be polarized at the instant of nuclear capture. For the longitudinal polarization, P_L, the muons can be unpolarized but the recoil direction must be controlled. For the transverse component, P_T, both the nonzero muon polarization and the recoil direction measurement must be provided. In order to fulfil the above conditions we utilize the stack-target technique developed in the investigation of the muon capture on ^{12}C [8]. The longitudinally polarized muons are stopped in the target material. Some of them form muonic atoms with target nuclei. These atoms disintegrate via

two competing processes: decay of muons or nuclear capture. If the final nucleus in the capture process is β-active the vector component of the nuclear polarization can be measured via β-asymmetry originating from parity violation in weak interactions. This method is feasible if the nuclear polarization can be preserved for a time period longer than the β-decay time. This can be accomplished by applying an external magnetic field (decoupling of dipole interactions) and embedding the recoiling nuclei into an environment with zero electric field gradient to avoid quadrupole interactions. In order to gain control over the recoil direction, a thin layer of the target material is sandwiched between polarization preserving and destroying materials (Fig. 1). In this way most of the recoiling nuclei are stopped outside the target material. The observed β-asymmetry is then due to the decay
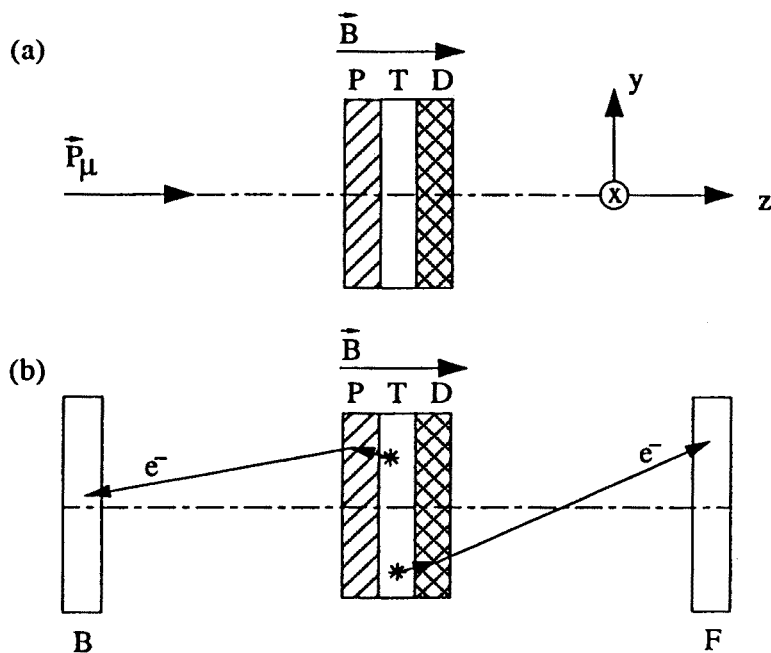

Fig. 1. Principle of the measurement, (a) — irradiation, (b) — asymmetry counting. The magnetic field $\vec{B}$ is parallel to the muon beam axis (and muon spin polarization). One sandwich consists of the polarization maintaining layer P, production layer T and depolarizing layer D. F and B designate β-asymmetry detectors.

of nuclei stopped exclusively in the polarization preserving material. Those stopped in the polarization destroying layer and in the target itself generate isotropic β-decay distributions. By averaging over the recoil direction it is easy to show that for an infinitesimally thin target the polarization signal

changes between

$$\langle P \rangle_{\mathrm{F}} = \tfrac{1}{2} \cdot P_{\mathrm{av}} + \tfrac{1}{4} \cdot P_{\mathrm{L}} \tag{10}$$

and

$$\langle P \rangle_{\mathrm{B}} = \tfrac{1}{2} \cdot P_{\mathrm{av}} - \tfrac{1}{4} \cdot P_{\mathrm{L}}. \tag{11}$$

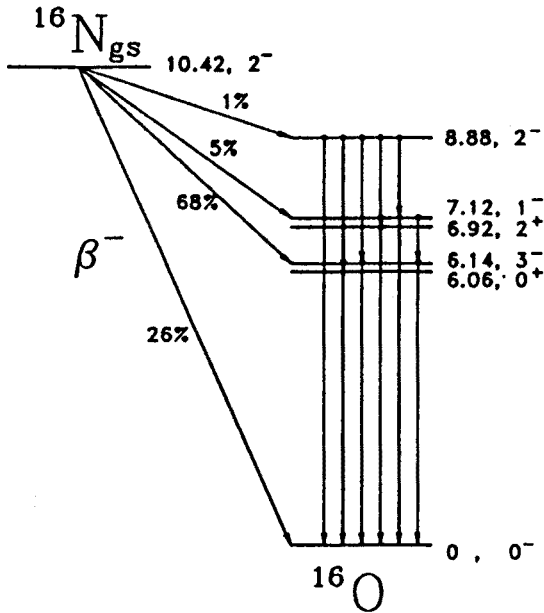when the positions of P and D layers are interchanged.

Fig. 2. Transition scheme between ^{16}O and ^{16}N.

The relevant formula for the angular distribution of electrons from β-decay of oriented nuclei can be written as:

$$W(\theta, E) \propto 1 + P \cdot a_1 \cdot f_1(E) \cdot P_1(\cos\theta) + A \cdot a_2 \cdot f_2(E) \cdot P_2(\cos\theta), \tag{12}$$

where P (A) are the nuclear vector polarization (alignment); a_1, a_2 are the vector and tensor analyzing power parameters, respectively. $f_i(E)$ represent the energy dependences and $P_i(\cos\theta)$ are Legendre polynomials where θ is the polar angle with respect to the axis of nuclear orientation. The ground state of ^{16}N decays mainly via two transitions (see Fig. 2; β^- branching ratios and energy levels are taken from [14]):

$$^{16}\mathrm{N}_{\mathrm{gs}} \rightarrow {}^{16}\mathrm{O}_{3^-}, \quad 68\%, \quad E_{\mathrm{max}}^{\mathrm{kin}} = 4.28\,\mathrm{MeV}\ (E_0 = 9.4)\ , \tag{13}$$

$$^{16}\mathrm{N}_{\mathrm{gs}} \rightarrow {}^{16}\mathrm{O}_{0^+}, \quad 26\%, \quad E_{\mathrm{max}}^{\mathrm{kin}} = 10.42\,\mathrm{MeV}\ (E_0 = 21.4)\ . \tag{14}$$

E_0 is the maximum total energy of electrons (in electron mass units). Since the first transition is allowed and the second one 1st-forbidden we have [15]:

$$a_1^{(1)} = 2/3, \ a_2^{(1)} \approx 0, \qquad\qquad f_1^{(1)} = v/c, \qquad\qquad (15)$$

$$a_1^{(2)} = 0, \qquad a_2^{(2)} = -\sqrt{7/10}, \qquad f_2^{(2)} = \frac{(E^2 - 1)}{[E^2 - 1 + (E_0 - E)^2]}, \quad (16)$$

where v, E are the velocity and total energy of the electrons, respectively. The counting rate asymmetries shown by the forward (F) and backward (B) detectors when the target is flipped by $180°$ about the x-axis (Fig. 1) are:

$$\langle ASY \rangle_{\mathrm{F}}^{(1)} = \frac{1}{6} \cdot \frac{+P_{\mathrm{L}} \cdot f_1^{(1)}}{1 + \frac{1}{3} \cdot P_{\mathrm{av}} \cdot f_1^{(1)}},$$

$$\langle ASY \rangle_{\mathrm{B}}^{(1)} = \frac{1}{6} \cdot \frac{-P_{\mathrm{L}} \cdot f_1^{(1)}}{1 - \frac{1}{3} \cdot P_{\mathrm{av}} \cdot f_1^{(1)}} \qquad (17)$$

for the first transition. Thus, from the above asymmetries, P_{av} and P_{L} can be deduced.

For a measurement of P_{T} the holding field must be oriented perpendicularly to the muon spin. The formulas for the corresponding β-asymmetry signals can be found elsewhere [16] and will not be further discussed here.

3.2. Beam and irradiation unit

The experiment was performed at the μE4 beam line of the meson factory at the Paul Scherrer Institute (PSI) in Villigen, Switzerland. Longitudinally polarized negative muons ($P_\mu \approx 0.7$) with a momentum of 50 MeV/c, and average rate of $10^6 \, \mathrm{s}^{-1}$ were focused on the target (Fig. 3). The typical beam spot had ~ 6 cm FWHM. The activation unit was equipped with a beam intensity monitor: 2 mm thick plastic scintillator (δ_μ), and a Michel-electron monitor: two 2 mm thick plastic scintillators (δ_{M}, Δ_{M}) in coincidence which served to adjust the thickness of the muon energy degrader (D) in order to obtain the maximum muon stop rate in the target. The background produced by the beam was reduced by shielding the muon channel and by switching off the beam during the β-asymmetry counting phase. This was accomplished by means of a mechanical chopper moving a 5 cm thick copper plate into the muon channel.
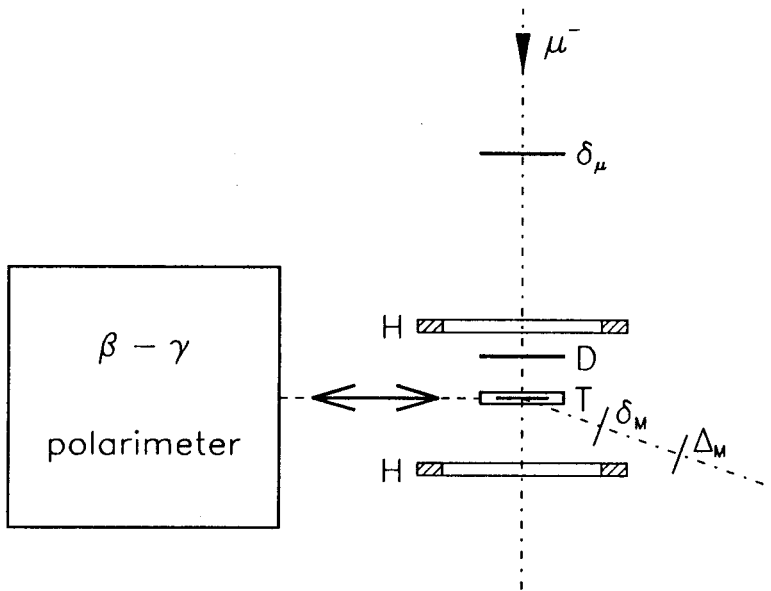
Fig. 3. Layout of the experiment. δ_μ, δ_M, Δ_M - plastic scintillators, H — Helmholtz coils, D — energy degrader, T — target cryostat. Horizontal arrows indicate the direction of movement of the target between the activation unit and the β-γ-polarimeter.

3.3. Targets

The oxygen rich target material we used was TiO_2. This compound is expected to depolarize negative muons and thus, according to Eqs. (3) - (5), the measurement was sensitive to P_L only. This oxide was chosen mainly because the necessary technology to prepare thin TiO_2-layers is well understood. Our choice for the polarization preserving material was metallic palladium. According to the results of Refs. [11–13] the estimated polarization relaxation time for ^{16}N nuclei implanted into palladium at liquid helium temperature is about 30 s. Aluminium was used as the polarization destroying material. The thickness of the TiO_2 layer was optimized such that most of the ^{16}N nuclei with recoil energy about 300 keV could leave the target layer while preserving an acceptable ^{16}N production rate. The thicknesses of palladium and aluminium layers was determined by the stopping range of ^{16}N nuclei in these metals. The resulting thicknesses of the sandwich layers ($Pd/TiO_2/Al$) were 5000 Å, 2000 Å and 8000 Å, respectively. The target sandwiches were produced using the sputtering equipment at the PSI. In order to gain in overall efficiency of the experiment, 130 sandwiches were stacked together. The stack target was mounted in the liquid-helium

cryostat and cooled down to 6 K. The cryostat had 0.1 mm thick phosphor-bronze windows and its design allowed fast movement of the target between the activation unit and the β-polarimeter. Targets were kept in a uniform magnetic field of 50 gauss with $\vec{B}$ parallel to the beam and polarimeter axes.

For test and calibration purposes we used both, a dummy stack target with TiO_2 replaced with metallic Ti and a water target consisting of 2–5 mm thick layer of water contained between thin Kapton foils. The dummy stack target was used to study the oxygen contamination of the Pd and Al layers. For μ^--capture experiments H_2O serves as a pure oxygen target and thus provides almost background free β- and γ-spectra from ^{16}N-decay — ideal for detector calibrations.

3.4. β-polarimeter

The ^{16}N nucleus in the ground state is well suited for a measurement of its polarization by detecting β-decay asymmetry. However, one of the main problems in measuring this asymmetry is the intense fake β-activity induced by the capture of muons in materials other than ^{16}O. Since the capture rate is roughly proportional to Z^4 and the target and its surrounding must contain many high-Z elements (Pd, Cu, Al, Fe), the resulting β-rate from ^{16}N-decay is only about 1 per mil of the total rate emitted from the target body. The most affected is the 4.28 MeV β-transition which is crucial for a measurement of the vector component of the nuclear polarization. Fortunately this transition is followed by the 6.14 MeV γ-transition between the 3^- and 0^+ states of ^{16}O (Fig. 2). Since such high energy γ-rays are rare, the β-γ–coincidences (with the low γ-energy threshold at about 4–5 MeV) provides a powerful condition for suppressing the fake β-activities. Obviously, an high efficiency of γ-ray detectors is of paramount importance for practical implementations.

Our β-polarimeter consisted of two electron telescopes covering about 20 % of the total solid angle. Each of the detectors consisted of three plastic scintillators (1 mm, 3 mm and 50 mm thick, respectively). They were surrounded by 64 BGO crystals for γ-detection as shown in Fig. 4. The BGO array was arranged in four planes covering roughly 70 % of the full solid angle. All the polarimeter detectors, including the BGO-walls, were installed in an aluminium housing with entrances for the target cryostat and Helmholtz coils.
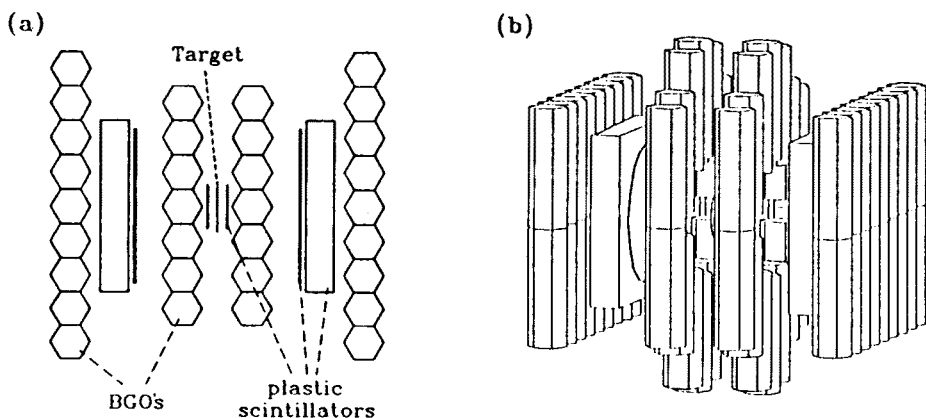
(a)   **(b)**

Target

BGO's   plastic
             scintillators

Fig. 4. Layout of detectors in the β-polarimeter: (a) — top view, (b) — perspective view.

3.5. Electronics and data acquisition

The main tasks assigned to the electronics and the data acquisition system were: (i) counting events in the muon-beam monitor and in the Michel-electron monitor, (ii) recognition and registration of the β-polarimeter events and (iii) control of auxiliary devices.

The pulses from the beam and Michel-electron monitors were sent to discriminators. Logic signals from these discriminators as well as coincidences between the two detectors of the Michel-electron telescope were counted by scalers.

Read-out of the β-polarimeter events included information about energies of all registered particles and about relative times between the detection of the electron in the β-telescope and of the coincident γ-ray in the BGO system. A schematic diagram of the electronics is presented in Fig. 5. Anode outputs of all photomultipliers (PM's) were directly coupled to inputs of linear Fan-In/Fan-Out units (FO). The pulses from PM's attached to the same thick E-scintillator were added. Then the pulses of all counters were split into two: one passing through delays to a FERA ADC (FERA 0), the other sent to a discriminator and subsequently into a logic section of the electronics. The trigger signal was produced by the computer-controlled OR of triple coincidences between the two thin (δ, Δ) and the stopping E-detectors for both β-telescopes. Within a given time window (150 ns) the pulse height and time interval (relative to the trigger signal) of all responding polarime-

Fig. 5. Schematic diagram of the polarimeter electronics.

ter detectors were digitized and acquired into the FERA system. Charge sensitive ADC's and Time-to-FERA converters (TFC's) were used for this purpose.

3.6. Measurement cycle

The measurement cycle was divided into two phases: activation of the target and counting in the β-polarimeter. They were separated by the time interval necessary for the transport of the target between the two positions. The chosen number of cycles was grouped into a so-called supercycle, characterized by the same target orientation with respect to the muon spin direction. The supercycles were separated with a longer pause, about 3 seconds, during which the target together with the cryostat was rotated by 180°. In this way the orientation of the stack target in two consecutive supercycles was reversed.

Activation and measurement periods were divided into 64 time channels. Typically we measured with channels of 160 ms duration and a supercycle consisting of 5 cycles.

Background measurements were performed under the same conditions as runs with the regular target. The background runs were performed with the cryostat containing an empty target frame in order to obtain the global intensity of the background originating in any source other than the stack target itself.

For reference, the measurements were repeated with the target at room temperature. Any asymmetry observed in such conditions would be instrumental in origin since the polarization relaxation time is shorter than 1 s, *i.e.* much less than the duration of the counting period.

The whole measurement process was controlled by two microprocessors communicating via the CAMAC dataway. The event data stream was directed to the back-end computer (VAXstation 4000/90) and stored for off-line analysis.

4. Performance of polarimeter

4.1. Calibration of β-telescopes

The performance of the β-telecopes was checked in the measurements with a water target. The theoretical β-energy distributions of the three most significant β-transitions were convoluted with the instrumental resolution of the plastic detectors. The energy loss and energy- and angular-straggling effects for electrons on their way between the target and the thick detector were taken into account. The calibration parameters (*e.g.* the energy dependence of the resolution function) were obtained by studying the spectra taken with radiation sources. Only small adjustments to these parameters (primarily detector gains) were necessary to reproduce the β-spectra from the decay of ^{16}N. Fig. 6 shows a fit to the experimental spectrum where the overall normalization and the relative abundance of 4.28 MeV and 10.42 MeV transitions were free parameters. From this result it is concluded that the β-telescopes performed very well.
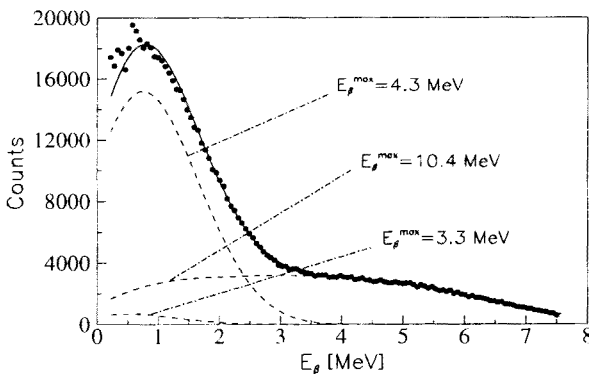

Fig. 6.   β-spectra collected with the water target — decomposition into β-transitions. The instrumental resolution was included in the fit procedure.

4.2. BGO-detectors

Energy calibration of the BGO detectors was based on the 6.14 MeV γ-peak ($3^- \to 0^+$ transition in ^{16}O). The events from the detectors for which this peak could not be clearly identified were rejected from further analysis. The calibration of the TFC/ADC system was performed during the testing phase before the run by measurements with fixed (cable) delays at the TFC inputs.

In order to check the performance of the γ-detection system and to prepare selection criteria for sorting the β-γ-coincidence events, the spectra of energy and coincidence time were built separately for each BGO detector, with the requirements of a triple coincidence in one of the β-telescopes (trigger) and of both ADC and TDC non-zero conversions for a given BGO.
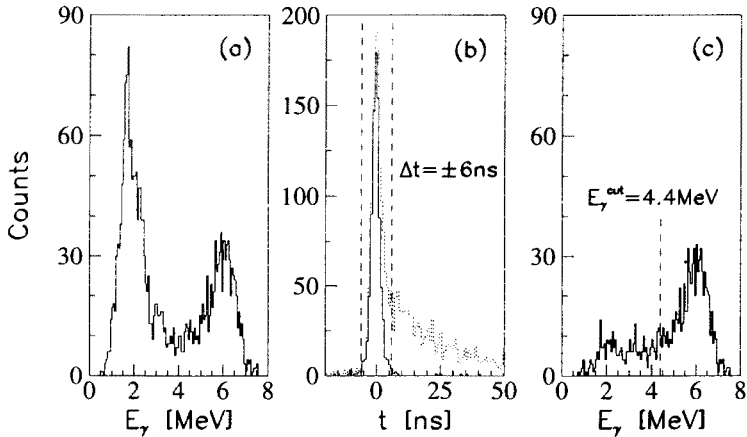
Fig. 7. Example of the gamma-spectra for a BGO crystal: (a) — energy spectrum of γ-rays coincident with any electron in the β-telescopes, (b) — time spectra of the same BGO prompt coincidence peak (solid line) and all events (dotted line), (c) — same as (a) but gated by the time window indicated in (b). The dashed line in (c) represents the energy threshold applied in the further analysis of the β-γ-coincidences.

In general, the detectors performed very well. The total absorption peak for the 6.14 MeV gammas was clearly visible in their energy spectra (Fig. 7a). Time spectra of these detectors reveal well defined prompt coincidence peaks with only a small contribution from delayed coincidences (Fig. 7b). This contribution, arising from fake activities induced by μ-capture in elements heavier than ^{16}O, vanishes when events with an energy deposition in the BGO crystals lower than the energy threshold at about 4.4 MeV are rejected.

Similarly, selecting the prompt coincidence region (± 6 ns around the prompt peak centre) as the event selection criterion, one obtains the BGO energy spectra with the low-energy background significantly reduced (see Fig. 7c). Generally, a lower rate of interesting events was registered in the outside BGO walls. This effect can be attributed to the smaller solid angle covered by these detectors and their shadowing by other detectors.

4.3. γ-multiplicity

We have investigated the γ-multiplicity for the β-γ-coincidence events. If no cuts had been set in the BGO spectra, at least two γ's would had been registered in about 10% of events. After selection of the prompt coincidences the contribution from the multiple-γ-events was reduced to about 3%. Most of such events could be interpreted as one γ depositing its energy in two adjoining BGO crystals via Compton scattering or pair production. Since for the majority of γ-rays, energy deposition takes place in only one crystal, our analysis could treat each BGO detector individually, without the necessity for cluster recognition.

4.4. Single and coincidence β-spectra

Events registered in the β-telescopes during the measurements with the stack targets, the water target and the target frame alone (background measurement), were subjected the same analysis procedure. For the single β-spectra we required ADC conversions for all three detectors of the given β-telescope. For the β-γ-coincidence spectra two additional conditions were imposed: the β-γ-coincidence time had to fall into the prompt-coincidence time window and the energy deposited in one of the BGO detectors had to be higher than 4.4 MeV.

The single and coincidence β-energy spectra for the water target are presented in Fig. 8. Using the already described decomposing procedure, the contribution from the 10.42 MeV transition, which is not followed by a γ-ray, was identified in the single β-spectrum. Comparing the low energy parts of the single and coincidence spectra one obtains the efficiency of the β-γ-coincidences to be about 20 %.

Single and coincidence β-energy spectra for the Pd/TiO$_2$/Al stack target are presented in Fig. 9a. The coincidence spectrum has been renormalized to account for the efficiency of β-γ-coincidences. A high selectivity of the polarimeter for the 4.3 MeV transition from the ^{16}N nuclei can be seen. In order to check the purity of the spectrum, the decay time for the β-γ-coincidences was fitted (Fig. 9b). The result (10.3 ± 0.4) s is in excellent agreement with the lifetime of ^{16}N$_{gs}$ from the literature: (10.29 ± 0.03)s [17].
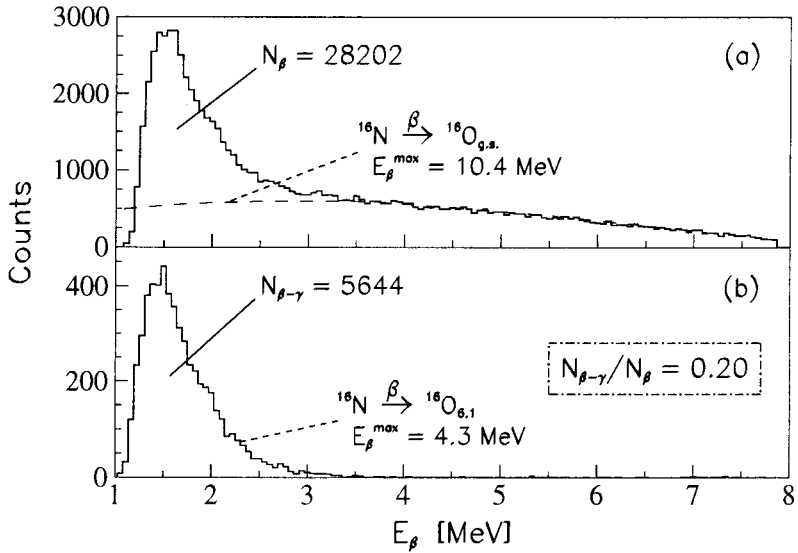
Fig. 8. β-spectra collected with the water target: (a) — single spectrum with the fitted contribution of transition with the endpoint energy of 10.42 MeV (dashed line), (b) — spectrum with the β-γ–coincidence requirement and appropriate cuts on the BGO time and energy. Note the disappearance of high energy events.
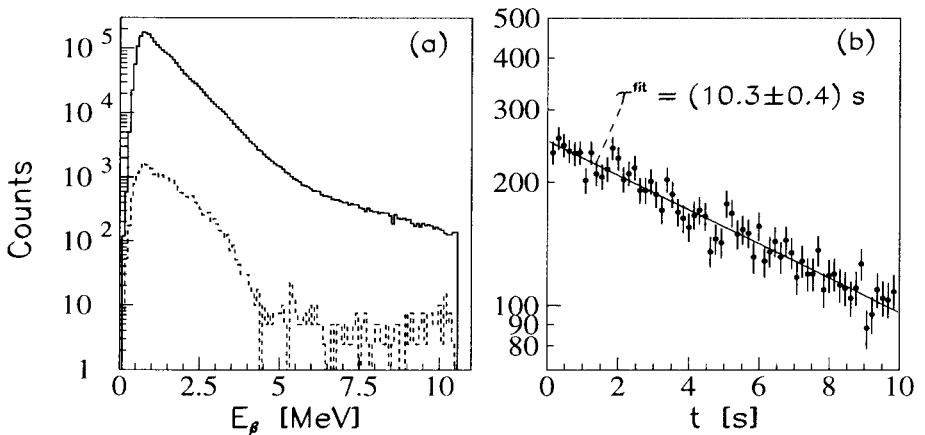

Fig. 9. β-spectra collected with the Pd/TiO$_2$/Al stack target (130 three-layers): (a) — single β-spectrum (solid line) and β-spectrum with the β-γ–coincidence requirement, appropriate time and energy cuts and corrected for the efficiency (dashed line), (b) — decay curve for the β-γ–coincidences with fitted life-time.

4.5. Asymmetry of β-γ-coincidences

The asymmetry in the β-γ-coincidences was determined using the conditions described above. Additionally, a requirement of long-term beam stability was necessary to avoid possible systematic effects.

The asymmetry was calculated separately for each run according to the formula:

$$ASY_i = \frac{N_i^{I} - N_i^{II}}{N_i^{I} + N_i^{II}}, \tag{18}$$

where I and II denote the target orientations, i — the telescope ($i = F, B$) and N_i^{I}, N_i^{II} are the numbers of β-γ-coincidences normalized to the number of muons in the corresponding activation phases. The results are presented in Fig. 10 for the measurements with the $Pd/TiO_2/Al$ target. The vertical dashed line separates the results of the measurements with the target cooled to 6 K (left side) and at room temperature (right side). Since no asymmetry is expected at room temperature (relaxation time < 1 s) the observed value is a measure of the geometrical imperfections of the experimental setup and serves as a reference for the measurement of the asymmetries at 6 K.
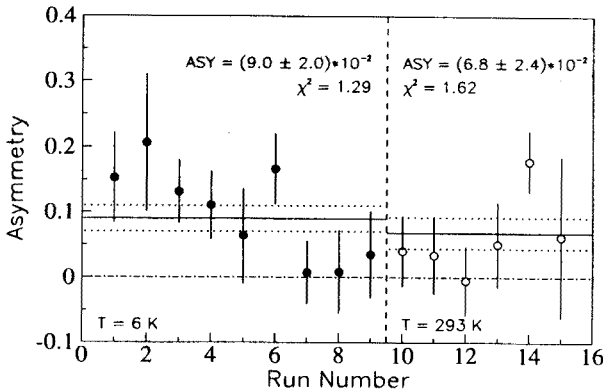

Fig. 10. Asymmetries of the β-γ-coincidences measured with the $PdTiO_2Al$ target (130 three-layers). The vertical dashed line separates the results of the measurements with the target cooled to 6 K (full points, left side) and at room temperature (circles, right side). The horizontal lines represent the mean values and one σ deviations.

Large error bars reflect the very limited statistics accumulated in this first measurement with the new polarimeter. The corrected result $ASY = 2.2 \pm 3.1$ is however consistent with the expectations. Based on theoretical calculations of P_L [18, 19] the estimated experimental β-asymmetry, which includes the most important instrumental effects, reaches 3–4 %.

5. Conclusions and outlook

The β-polarimetry technique which relies on the stack target principle, β-asymmetry measurement and the use of β-γ-coincidences with the subsequent γ-rays has been developed to measure the polarization observables of the $^{16}N_{gs}$ nuclei produced in the μ^--capture on ^{16}O. A prototype polarimeter has been built and successfully tested with the μ^--beam. It has a sufficient overall efficiency of about 4 % and very high background suppression power. Use of β-γ-coincidences seems to be compulsory to select in a clean way the β-transition of interest out of an almost three orders of magnitude larger fake β-background. Such a background cannot be avoided since it is inherently associated with the μ-capture reaction in the polarization preserving and destroying high Z materials used in the stack target.

The first β-asymmetry measurement performed with the new polarimeter did not produce conclusive results mainly due to the low counting statistics and still insufficient quality of the stack-target layers used in the measurement. Further measurements with improved targets, in particular, with a significantly larger number of three-layers, are foreseen. Measurements with oxides which provide nonzero muon polarization at the instant of capture (*e.g.* V_2O_5 [20]) are also planned. Such measurements will allow simultaneous access to P_L and P_{av}. The ratio P_L/P_{av} is less affected by systematic error and is thus better suited to deducing desired physical quantities such as the g_P/g_A ratio, discussed at the beginning of this paper.

REFERENCES

[1] J.H. Christenson, J.W. Cronin, V.L. Fitch, R. Turlay, *Phys. Rev. Lett.* **13**, 138 (1964).

[2] J.F. Donoghue, B.R. Holstein, G. Valencia, *Int. J. Mod. Phys.* **A2**, 319 (1987); K.F. Smith *et al.*, *Phys. Lett.* **B234**, 191 (1990); I.S. Altarev *et al.*, *Phys. Lett.* **B276**,242 (1992); J.P. Jacobs *et al.*, *Phys. Rev. Lett.* **71**, 3782 (1994).

[3] J. Sromicki, M. Allet, K. Bodek, W. Hajdas, J. Lang, R. Müller, S. Navert, O. Naviliat-Cuncic, J. Zejma, W. Haeberli, *Phys. Rev.* **C53**, 932 (1996).

[4] H. Burkhard, F. Corriveau, J. Egger, W. Fetscher, H.-J. Gerber, K.F. Johnson, H. Kaspar, H.J. Mahler, M. Saltzmann, F. Scheck, *Phys. Lett.* **160B**, 343 (1985).

[5] M. Ericson, *Prog. Part. Nucl. Phys.* **1**, 67 (1978).

[6] K. Kubodera, M. Rho, *Phys. Rev. Lett.* **67**, 3479 (1991).

[7] M. Lutz, S. Klimt, W. Weise, Meson Properties at Finite Temperature and Baryon Density, University of Regensburg, Report No. TPR-91-12.

[8] L.Ph. Roesch, V.L. Telegdi, P.A. Truttmann, A. Zehnder, L. Grenacs, L. Palffy, *Phys. Rev. Lett.* **46**, 1507 (1981); P.A. Truttmann, ETH dissertation 6753 (1981).

[9] W-Y.P. Hwang, H. Primakoff, *Phys. Rev.* **C16**, 397 (1977).

[10] M. Cyamukungu, PhD dissertation, Université Catholique de Louvain, 1991.

[11] J. Korringa, *Physica* **16**, 601 (1950).

[12] A. Proykova, L. Grenacs, *Nucl. Instrum. Methods* **A362**, 234 (1995).

[13] W. Wanderpoorten, private communication.

[14] D.R. Tilley, H.R. Weller, C.M. Cheves, *Nucl. Phys.* **A565**, 1 (1993).

[15] S.R. de Groot, H.A. Tolhoek, W.J. Huiskamp, *Alpha-, Beta- and Gamma-Ray Spectroscopy*, vol 2, ed. Kai Siegbahn, North-Holland Publ. Comp., Amsterdam 1965.

[16] A. Possoz, L. Grenacs, J. Lehmann, L. Palffy, J. Julien, C. Samour, *Phys. Lett.* **87B**, 35 (1979).

[17] F. Ajzenberg-Selove, *Nucl. Phys.* **A166**, 1 (1971).

[18] P.R. Subramanian, R. Parthasarathy, V. Devanathan, *Nucl. Phys.* **262**, 433 (1976).

[19] L. Mileshina, 1995, private communication.

[20] V.S. Evseev *et al.*, *JETP Lett.* **27**, 233 (1978).